Supporting information

Acidic pH-triggered AIE nanoparticles covalently cross-linking for enhanced tumor imaging and photodynamic therapy

Weiqi Zai, [a] Huiling Ji, [a] Jincheng Li, [a] Jing Wang, [a] Hongli Chen, [a] Dan Ding, [b] Shenglu Ji, *[a] and Nannan Wang *[a]

[a.] *The Key Laboratory of Biomedical Materials, School of Life Sciences and Technology, Xinxiang Medical University, Xinxiang 453003, China. E-mail: jishenglu@126.com, nannanwang@xxmu.edu.cn*

[b.] *Frontiers Science Center for New Organic Matter, State Key Laboratory of Medicinal Chemical Biology, Key Laboratory of Bioactive Materials, Ministry of Education, and College of Life Sciences, Nankai University, Tianjin 300071, China.*

1. Materials and instruments

1.1 Materials

ε-caprolactone (ε-CL) and stannous octoate ($Sn(Oct)_2$), N-acryloxysuccinimide (NAS), Hexane-1,6-dioldiacrylate (HDD) and 4,4'-trimethylene dipiperidine (TDP) were purchased from Adamas Reagent Co., Ltd (Shanghai, China). Potassium acetate, ammonium acetate and dibenzocyclooctyne-amine were Bide pharmatech co., ltd (Shanghai, China). 3-azidopropylamine was purchased from Jiangsu Aikon Biopharmaceutical R&D Co., Ltd. Chlorin e6, and 9,10-anthracenediyl-bis(methylene)dimalonic acid (ABDA) were purchased from Shanghai Macklin Biochemical Co., Ltd. Dihydrorhodamine 123 was purchased from Shanghai Yuanye Bio-Technology Co., Ltd. Hydroxyphenyl fluorescein (HPF) was purchased from Shanghai Maokang Biotechnology Co., Ltd. 2′,7′-Dichlorodihydrofluorescein diacetate (DCFH-DA) was purchased from Sigma-Aldrich.

1.2 Instruments

The synthesized compounds were characterized by ^{1}H NMR and ^{13}C NMR

(Bruker Ascend 400). HR-MS was conducted on a Bruker micrOTOF-Q III. UV-vis absorption spectra were recorded on a UV-26001 (Suzhou, China) at room temperature. Photoluminescence (PL) spectra were recorded on an Edinburgh FS5 fluorescence spectrophotometer. The zeta potentials of the prepared nanoparticles were measured on a zetasizer instrument (Nano ZS, Malvern). Morphology characterization of the nanoparticles was conducted via transmission electron microscopy (TEM, Hitachi H-7500, Japan).

2. Chemical synthesis

2.1 Synthesis of compound 2

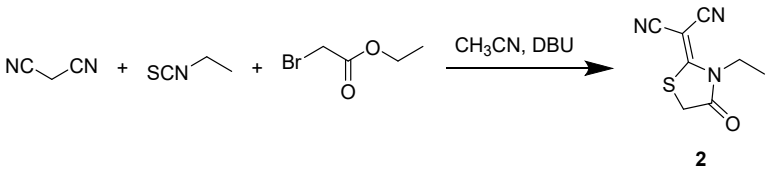

2

Scheme S1. The synthetic route for compound **2**.

Compound **2** was synthesized according to the literature.[1] Briefly, malononitrile (1.05 g, 15.9 mmol) was dissolved in acetonitrile (50 mL). Then ethyl isothiocyanate (1.5 g, 17.2 mmol) and 1,8-diazabicyclo[5.4.0]-7-undecene (DBU, 2.4 g, 15.7 mmol) were added dropwise to the reaction mixture in sequence. After stirring for 30 min at room temperature, ethyl bromoacetate (3 mL, 27 mmol) was added dropwise to the reaction mixture and further stirred for 1 h at room temperature. Then refluxed at 85°C for 3 h at N_2 atmosphere. After cooling to room temperature, the reaction mixture was condensed, acidified with 2 M HCl (42 mL), extracted with dichloromethane (DCM), washed with saturated saline solution, and dried over anhydrous Na_2SO_4. The crude product was condensed and purified by silica gel chromatography (pure petroleum ether (PE) to PE: ethyl acetate (EA) from 3:1→2:1, v:v) to get a pale yellow solid of compound **2** (yield: 2.45 g, 79.8%). ^{1}H NMR (400 MHz, Chloroform-*d*) δ 4.16 (q, *J* = 7.1 Hz, 2H), 3.99 (s, 2H), 1.33 (t, *J* = 7.2 Hz, 3H). ^{13}C NMR (101 MHz, Chloroform-*d*) δ 171.84, 171.56, 112.99, 111.79, 56.30, 40.68, 32.50, 13.98. HR-MS: calcd. $[M+H]^+$ = 194.0383; obsvd. $[M+H]^+$ = 194.0369.

2.2 Synthesis of TETCN

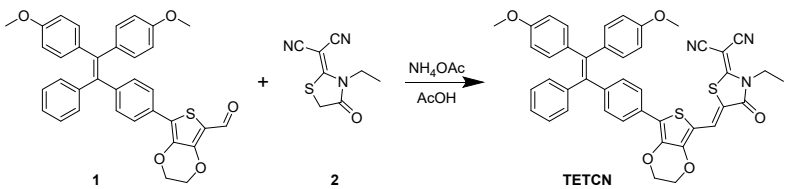

Scheme S2. The synthetic route for **TETCN**. Compound **1** was synthesized according to the literature.[2]

Compound **1** (337 mg, 0.6 mmol), compound **2** (347 mg, 1.8 mmol), and NH_4OAc (77 mg, 1.8 mmol) were dissolved in 12 mL of AcOH, then reacted at 120°C for 8 h under N_2 atmosphere. After cooling to room temperature, the reaction mixture was extracted with DCM, washed with saturated saline solution, and dried over anhydrous Na_2SO_4. The crude product was condensed and purified by silica gel chromatography (PE: EA = 10:1→1:1, v:v) to get a red solid of compound **TETCN** (yield: 300 mg, 67.8%). ^{1}H NMR (400 MHz, Chloroform-*d*) δ 8.12 (s, 1H), 7.57 (d, *J* = 8.1 Hz, 2H), 7.11 (s, 3H), 7.04 (m, 4H), 6.96 (dd, *J* = 16.5, 8.4 Hz, 4H), 6.65 (dd, *J* = 13.1, 8.5 Hz, 4H), 4.38 (m, 4H), 4.29 (d, *J* = 7.1 Hz, 2H), 3.75 (d, *J* = 5.5 Hz, 6H), 1.39 (t, *J* = 7.1 Hz, 3H). ^{13}C NMR (101 MHz, Chloroform-*d*) δ 166.10, 166.02, 132.76, 132.11, 131.58, 113.13, 65.30, 55.23, 40.61, 14.36. HR-MS: calcd. [M] = 735.1862; obsvd. [M] = 735.1879.

2.3 Synthesis of PCL-PEG

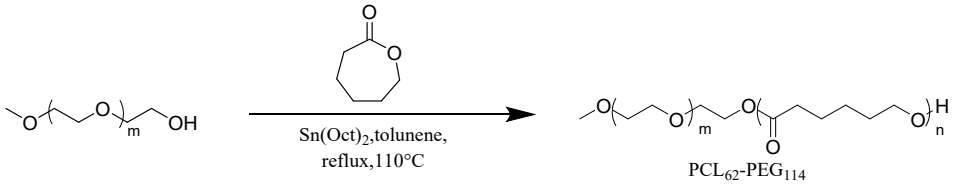

Scheme S3. The synthetic route for **PCL_{62}-PEG_{114}**.

PCL-PEG was synthesized according to the literature.[3] PEG_{114}-OH (2 g, 0.4 mmol), ε-CL monomer (3 g, 26.3 mmol) and a drop of $Sn(Oct)_2$ were dissolved in toluene (10 mL). After three cycles of freezing-degassing-thawing, the mixture was stirred at 110°C for 12 h. Then the solution was precipitated with excess ice ethyl ether and filtered to obtain the white solid product.

2.4 Synthesis of PCL_{60}-A and PCL-PAE-NAS

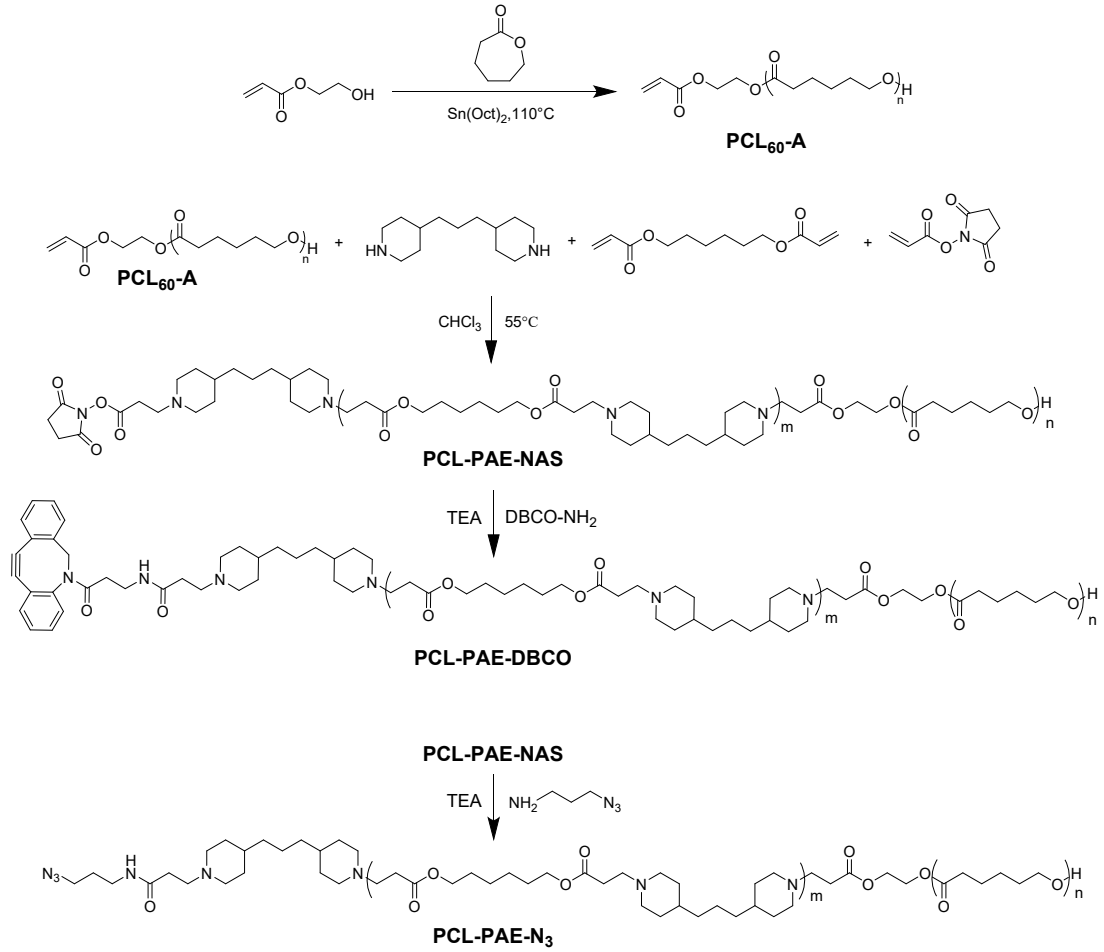

Scheme S4. The synthetic route for **PCL-PAE-NAS, PCL-PAE-DBCO and PCL-PAE-N_3**.

PCL-PAE-NAS was synthesized according to the literature.[3] Briefly, ε-CL (3 g, 26.3 mmol), HEA (50 mg, 0.43 mmol), and two drops of $Sn(Oct)_2$ were dissolved in 10 mL of toluene. After the reaction solution was fully dissolved, it was frozen, degassed and thawed three times, stirred at 110℃ for 12 h, precipitated with ice ether, vacuum filtered and dried to obtain PCL_{60}-acrylate (PCL_{60}-A) with a vinyl group at one end. Next, PCL_{60}-A (1.4 g, 0.047 mmol), Hexane-1,6-dioldiacrylate (HDD, 1.357 g, 0.84 mmol) and 4,4'-trimethylene dipiperidine (TDP, 1.352 g, 0.85 mmol) were dissolved in trichloromethane (10 mL). After dissolution, the reaction mixture was stirred at 55℃ for 3 days. Finally, N-acryloxysuccinimide (NAS, 67 mg, 0.094 mmol) was added to the mixture and the reaction was continued for 12 h. Then, the solution was precipitated into ice ethyl ether. Finally, the product obtained by suction filtration was dried under

vacuum to obtain PCL_{60}-b-PAE_{46}-NAS.

2.5 Synthesis of PCL-PAE-DBCO.

PCL_{60}-b-PAE_{46}-NAS (1 g) was dissolved in dimethyl sulfoxide (DMSO, 10 mL) and anhydrous chloroform ($CHCl_3$, 6 mL) in the reaction flask. Then DBCO-NH_2 (43.2 mg) was added, followed by triethylamine (TEA, 120 μL), and reacted at 35°C for 12 h. After that, the temperature was switched to 55°C for another 8 h of reaction. Subsequently, the solution was dialyzed against deionized water for 3 days (MWCO = 3500). Finally, PCL_{60}-PAE_{46}-DBCO was obtained by freeze-drying.

2.6 Synthesis of PCL-PAE-N_3.

PCL_{60}-PAE_{46}-N_3 was prepared by a method similar to PCL_{60}-PAE_{46}-DBCO. PCL_{60}-b-PAE_{46}-NAS (1 g) was dissolved in DMSO (10 mL) and anhydrous $CHCl_3$ (6 mL) in the reaction flask. Then 3-Azido-1-propanamine (15.6 mg) was added, followed by TEA (120 μL), and reacted at 35°C for 12 h. After that, the temperature was switched to 55°C for another 8 h of reaction. Subsequently, the solution was dialyzed against deionized water for 3 days (MWCO = 3500). Finally, PCL_{60}-PAE_{46}-N_3 was obtained by freeze-drying.

3. In vitro experiments

3.1 Preparation of PPP-DBCO and PPP-N_3 nanoparticles (NPs)

TETCN (1.5 mg), PCL-PEG (2.5 mg) and PCL-PAE-DBCO (1 mg) were dissolved in THF (1 mL). The solutions were added dropwise to 9 mL H_2O (pH 4.0) under sonication (300W, ultrasound for 9 s, pause for 1 s, for a total of 3 min). Subsequently, the solution was transferred to a dialysis bag (MWCO = 14000) and dialyzed for 24 h using ultrapure water (pH 7.0). The resulting solution was then concentrated using an ultrafiltration centrifuge tube to get **PPP-DBCO NPs** (1 mg/mL) and stored at 4°C.

PPP-N_3 NPs were prepared in a similar way, just replacing PCL-PAE-DBCO with PCL-PAE-N_3. The final concentration was also kept at 1 mg/mL.

3.2 Quantification of TETCN in PPP-DBCO and PPP-N_3 NPs

To determine the encapsulation efficiency (EE%) and drug loading (DL%) efficiency of TETCN in both NPs. Various concentrations of TETCN in water

(containing 1% THF) were prepared and their absorbance intensities were tested at 495 nm. By linear analysis, the standard curve of TETCN was built (y=0.0268x+0.0015, R^2=0.9999). Three batches of PPP-DBCO and PPP-N_3 were prepared according to the procedure of "3.1 Preparation of PPP-DBCO and PPP-N_3 nanoparticles". Through dialysis in ultrapure water (pH 7.0), unencapsulated TETCN diffused through the dialysis membrane into the external medium. Based on the absorbance of the external medium at 495 nm and the standard curve of TETCN, the EE% and DL% could be determined.

To test the release profile of TETCN in both NPs. The formed NPs were dialyzed in water at pH 6.5 and the absorbance of the external medium was tested to determine the released TETCN at different time points. Cumulative Release (%) = (Amount of TETCN released / Total of TETCN in NPs) × 100%

3.3 Acid pH-triggered NPs covalent aggregation detection

Prepare two small bottles containing stir bars, each bottle added PPP-DBCO (1 mg/mL, 200 μL) and PPP-N_3 (1 mg/mL, 200 μL). Adjust the pH of one bottle to 7.4 by adding sodium hydroxide, and adjust the pH of the other bottle to 6.5 by adding hydrochloric acid. Place both small bottles simultaneously in a 37°C constant-temperature magnetic stirrer and observe the changes in the solutions in the two bottles, record and take pictures.

3.3.1 TEM samples preparation: After stirring for 5 h, then diluted it twice under the same pH environment. 10 μL of the solution was dropped on a copper grid, let it stand for 10 min, and filter paper was used to absorb the excess solution. Then 5 μL of ultrapure water was dropped on the copper grid, let it stand for 1 min, and then used filter paper to absorb excess solution. The sample was dried overnight in a desiccator and then examined on a HITACHI TEM system. The individual PPP-DBCO or PPP-N_3 NPs TEM samples were prepared in the same way.

3.3.2 DLS and zeta potential detection: After stirring for 5 h, the samples were diluted 3-fold, and particle size and zeta potential were measured using a Nano ZS zetasizer. The individual PPP-DBCO or PPP-N_3 NPs TEM samples were prepared in the same way.

3.4 Detection of reactive oxygen species (ROS) in PBS solution

3.4.1 The detection of total ROS: 2, 7-dichlorodihydrofluorescein (DCFH) was prepared by hydrolyzing 2, 7-dichlorodihydrofluorescein diacetate (DCFH-DA) with 10 mM NaOH for 30 min and then neutralized with PBS to obtain a stock solution (50 μM).[4] Then, PBS solutions of TETCN (10 μM), Ce6 (10 μM), PPP-DBCO (10 μM, calculated based on TETCN) or PPP-N_3 (10 μM, calculated based on TETCN) in the presence of DCFH (5 μM) were prepared and irradiated under white light irradiation (0.1 W cm^{-2}) for different times, and the fluorescence spectra were measured under 488 nm excitation.

To detect the total ROS of mixed PPP-DBCO + PPP-N_3 at pH 7.4 or 6.5, PPP-DBCO and PPP-N_3 were mixed in equal volumes, with a final concentration of TETCN at 10 μM. Then add DCFH, lighting and record the spectra of DCFH in the same way.

3.4.2 The detection of hydroxyl radicals (·OH): PBS solutions of TETCN (10 μM), Ce6 (10 μM), PPP-DBCO (10 μM, calculated based on TETCN) or PPP-N_3 (10 μM, calculated based on TETCN) in the presence of hydroxyphenyl fluorescein (HPF, 5 μM) were prepared and irradiated under white light irradiation (0.1 W cm^{-2}) for different times, and the fluorescence spectra of HPF were collected under 490 nm excitation.

To detect the ·OH of mixed PPP-DBCO + PPP-N_3 at pH 7.4 or 6.5, PPP-DBCO and PPP-N_3 were mixed in equal volumes, with a final concentration of TETCN at 10 μM. Then add HPF, lighting and record the spectra of HPF in the same way.

3.4.3 The detection of superoxide anion ($O_2^{\cdot-}$): PBS solutions of TETCN (10 μM), Ce6 (10 μM), PPP-DBCO (10 μM, calculated based on TETCN) or PPP-N_3 (10 μM, calculated based on TETCN) in the presence of dihydrorhodamine 123 (DHR 123, 5 μM) were prepared and irradiated under white light irradiation (0.1 W cm^{-2}) for different times, and the fluorescence spectra of DHR123 were collected under 500 nm excitation.

To detect the $O_2^{\cdot-}$ of mixed PPP-DBCO + PPP-N_3 at pH 7.4 or 6.5, PPP-DBCO and PPP-N_3 were mixed in equal volumes, with a final concentration of TETCN at 10 μM. Then add DHR123, lighting and record the spectra of DHR 123 in the same way.

3.4.4 The detection of singlet oxygen ($^1O_2$): PBS solutions of TETCN (10 μM), Rose Bengal (RB, 10 μM), PPP-DBCO (10 μM, calculated based on TETCN) or PPP-N_3 (10 μM, calculated based on TETCN) in the presence of ABDA (50 μM) were prepared and irradiated under white light irradiation (0.1 W cm^{-2}) for different time, and the absorption spectra were collected between 300-450 nm.

To detect the $^1O_2$ of mixed PPP-DBCO + PPP-N_3 at pH 7.4 or 6.5, PPP-DBCO and PPP-N_3 were mixed in equal volumes, with a final concentration of TETCN at 10 μM. Then add ABDA, lighting and record the absorption spectra between 300-450 nm in the same way.

3.5 Cellular uptake and visualization of fluorescence signals

PPP-DBCO (1 mg/mL, 200 μL), PPP-N_3 (1 mg/mL, 200 μL), and PPP-DBCO (1 mg/mL, 100 μL) + PPP-N_3 (1 mg/mL, 100 μL) were placed in a bottle, respectively. HCl was added to the above solutions to adjust the pH to 6.5 and stirred for 2 h at 37°C to initiate crosslinking. Then, the above various NPs were diluted to 20 μM using RPMI 1640 medium (pH 6.5) and incubated with 4T1 cancer cells for 8 h. Following incubation, the cells were thoroughly rinsed with PBS to remove residual nanoparticles, fixed with 4% paraformaldehyde (PFA) at 37°C for 30 minutes in the dark, and rinsed again. Cellular fluorescence was subsequently visualized and imaged using a confocal laser scanning microscope (CLSM).

3.6 Intracellular ROS detection

4T1 cells were seeded in 96-well plates at a density of 1×10^4 cells per well and cultured for 24 h. The cells were then treated with PPP-DBCO, PPP-N_3, or PPP-DBCO + PPP-N_3 at a concentration of 20 μM in a pH 6.5 medium. The experimental groups included: Control, Control + L, PPP-DBCO, PPP-DBCO + L, PPP-N_3, PPP-N_3 + L, PPP-DBCO + PPP-N_3, and PPP-DBCO + PPP-N_3 + L. After 10 h of incubation, the medium was removed, and the cells were gently rinsed twice with PBS to eliminate residual nanoparticles. Subsequently, 100 μL of serum-free 1640 medium containing 10 μM DCFH-DA was added to each well, followed by incubation at 37°C in the dark for 30 minutes. The cells were washed again with PBS and subjected to white light irradiation (0.1 W cm^{-2}, 5min). Fluorescence was immediately observed and captured

using an inverted fluorescence microscope.

3.7 Cytotoxicity Study

4T1 cells were seeded into 96-well plates at a density of 1×10^4 cells/ well, and cultured in a 37°C incubator for 24 h. PPP-DBCO, PPP-N_3, and PPP-DBCO + PPP-N_3 were stirred in medium with a pH of 6.5 to form large aggregates. Then all the NPs were diluted to 40 μM, 20 μM and 10 μM, and incubated with 4T1 cells for 10 h. After being washed with fresh RPMI 1640 medium, 4T1 cells with different treatments were exposed to white light irradiation (0.2 W cm^{-2}) or not for 4 min and continued incubation for 12 h. Then cells were incubated with 0.5 mg/mL methylthiazolyldiphenyl-tetrazolium bromide (MTT) in RPMI 1640 at 37°C for 4 h. Subsequently, the solution was discarded, and 100 μL of DMSO was added to each well, dissolved and assayed using a microplate reader at 570 nm.

3.8 Hemolysis test

Take blood from the eyes of mice, add heparin for anticoagulation, then add an appropriate amount of PBS and mix evenly. Centrifuge at 2000 rpm for 5 min and repeat the above operation three times. Finally, add an appropriate amount of PBS to disperse it. The experiment was divided into NPs, positive control (used water) and negative control (used PBS). In order to subtract the fluorescence of AIE NPs, the group with NPs but no blood cells was also prepared. The samples were incubated in a 37°C water bath for 2 h. After 2 h, the blood was subjected to 10,000 rpm for 5 min. The samples were placed on the same horizontal line, and photos were taken with a mobile phone. 100 μL of the samples was placed in a 96-well plate and assayed using a microplate reader at 570 nm. The haemolysis rate = $\frac{OD(NPs + blood\ cells) - OD(NPs)}{OD(positive) - OD(negative)}$

3.9 In vivo time point imaging

The 6-week-old female BALB/c mice were from Henan Skobes Biotechnology Co., Ltd. All animal procedures were performed following the Guidelines for Care and Use of Laboratory Animals of Xinxiang Medical University and approved by the Animal Ethics Committee of Xinxiang Medical University.

To establish 4T1 tumor-bearing mouse model, 4T1 cells were cultured in vitro and

harvested during the logarithmic growth phase. After centrifugation, the cells were resuspended in PBS at a density of 1×10^7 cells per milliliter. Subsequently, 100 μL of the cell suspension was injected into the subcutaneous tissue of the right posterior buttock of each mouse. When the tumor volume reached approximately 100 mm^3, 4T1 tumor-bearing mice were randomly divided into 3 groups: PPP-DBCO, PPP-N_3, and PPP-DBCO + PPP-N_3. After intravenous injection of PPP-DBCO (1 mg/mL, 200 μL), PPP-N_3 (1 mg/mL, 200 μL), and PPP-DBCO (1 mg/mL, 100 μL) + PPP-N_3 (1 mg/mL, 100 μL), respectively. The mice were imaged using BV100 imaging system at 1, 2, 4, 8, 12 and 24 h time points with a 520 nm laser for excitation. Then, the main organs and tumors of the mice were isolated and imaged using BV100 imaging system.

3.10 Tumor suppression study.

The establishment of the mouse tumor model is the same as above. When the tumor volume reached approximately 80 mm^3, 4T1 tumor-bearing mice were randomly divided into five groups: PBS, PPP-DBCO + L, PPP-N_3 + L, PPP-DBCO + PPP-N_3, and PPP-DBCO + PPP-N_3 + L. After intravenous injection of PBS (200 μL), PPP-DBCO (1 mg/mL, 200 μL), PPP-N_3 (1 mg/mL, 200 μL), PPP-DBCO (1 mg/mL, 100 μL) + PPP-N_3 (1 mg/mL, 100 μL), and PPP-DBCO (1 mg/mL, 100 μL) + PPP-N_3 (1 mg/mL, 100 μL), respectively. Tumors were exposed to white light irradiation (0.5 W cm^{-2}, 10 min). The tumor volume and body weight were measured every two days. The tumor volume was calculated by using the formula: $V = L\times W\times W/2$ (L, the longest dimension; W, the shortest dimension). The mice were sacrificed 14 days after the final laser treatment. The major organs (heart, liver, spleen, lung and kidney) and tumor were harvested, fixed in 4% paraformaldehyde, embedded in paraffin, sliced and stained with hematoxylin and eosin (H&E). Immunofluorescence staining of TdT-mediated dUTP nick-end labeling (TUNEL) and Ki67 was performed on tumor tissues.

3.11 Data analysis

Data were expressed as mean ± standard deviation from triplicate experiments performed in a parallel manner. Comparison between more than two groups was conducted with one-way ANOVA by using GraphPad Prism 7.0. A difference of $p < 0.05$ was considered statistically significant.

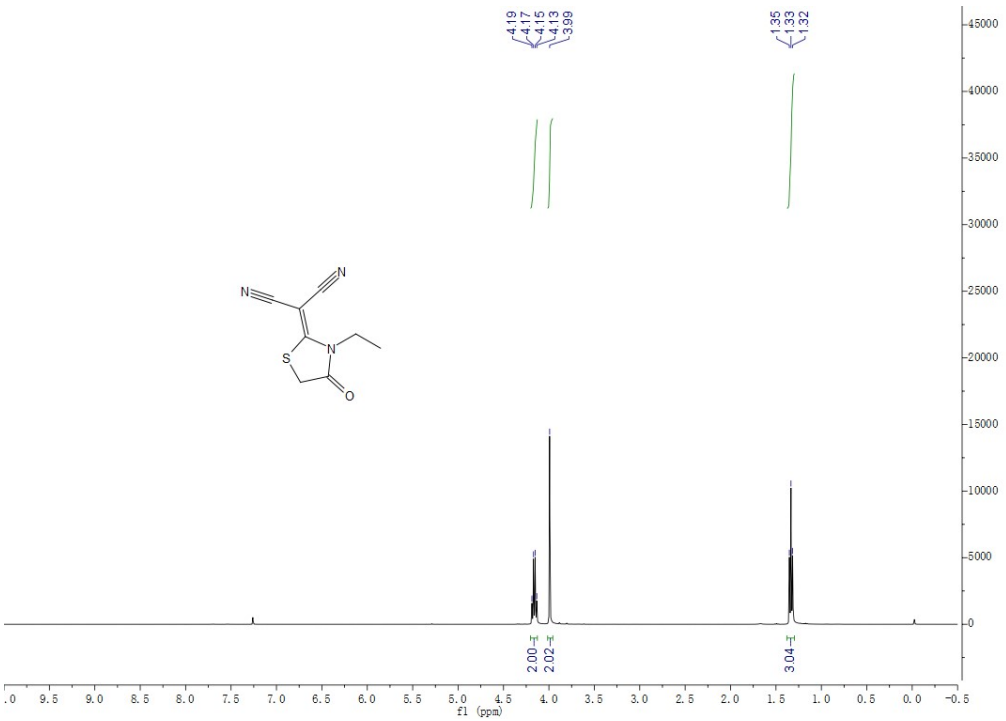

Figure S1. ^{1}H NMR spectrum of **RCN-C2**.

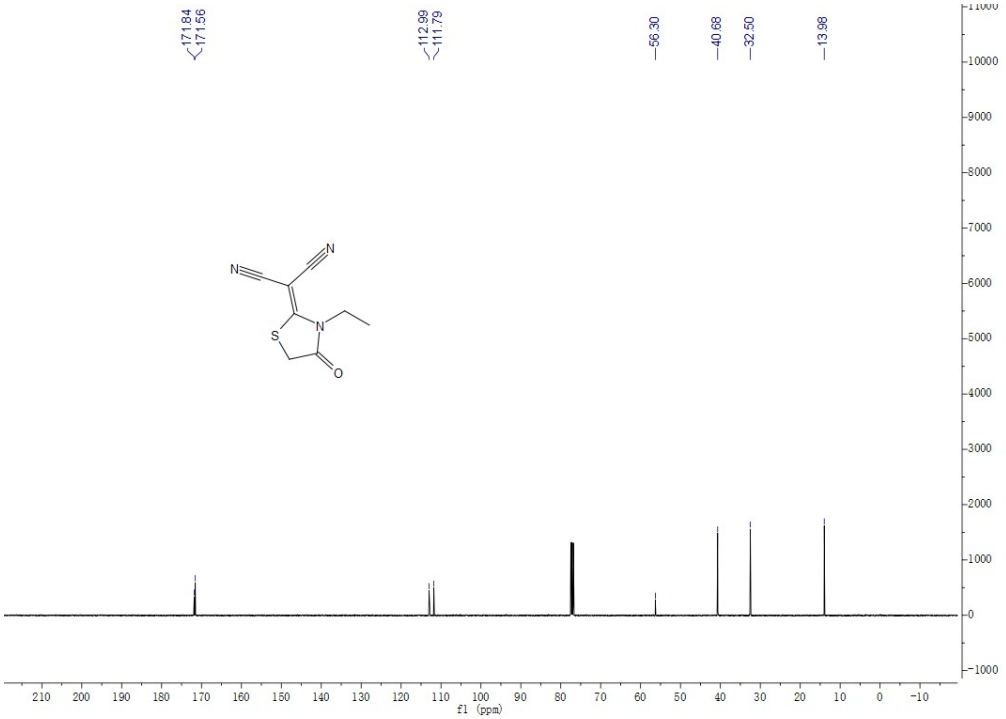

Figure S2. ^{13}C NMR spectrum of **RCN-C2**.

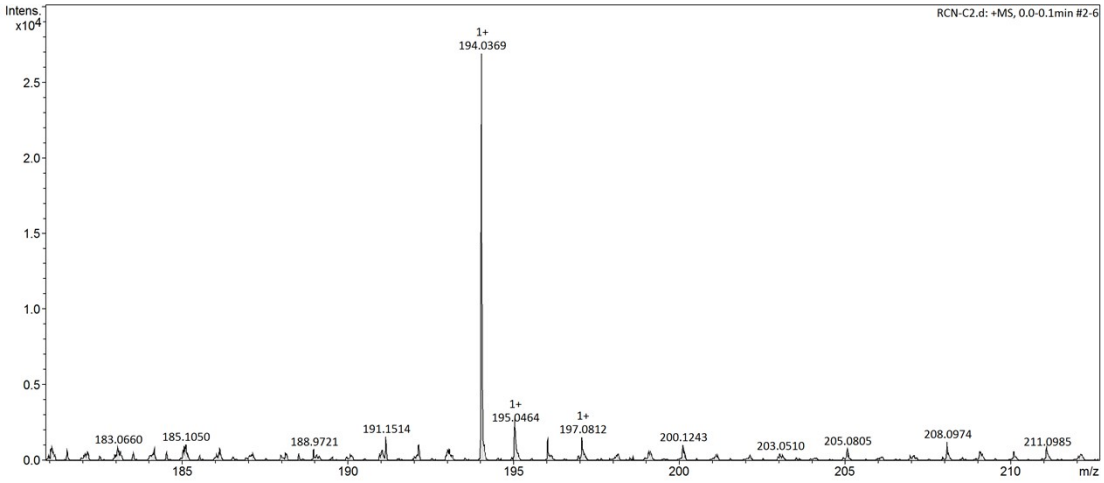

Figure S3. HR-MS spectrum of R**CN-C2**.

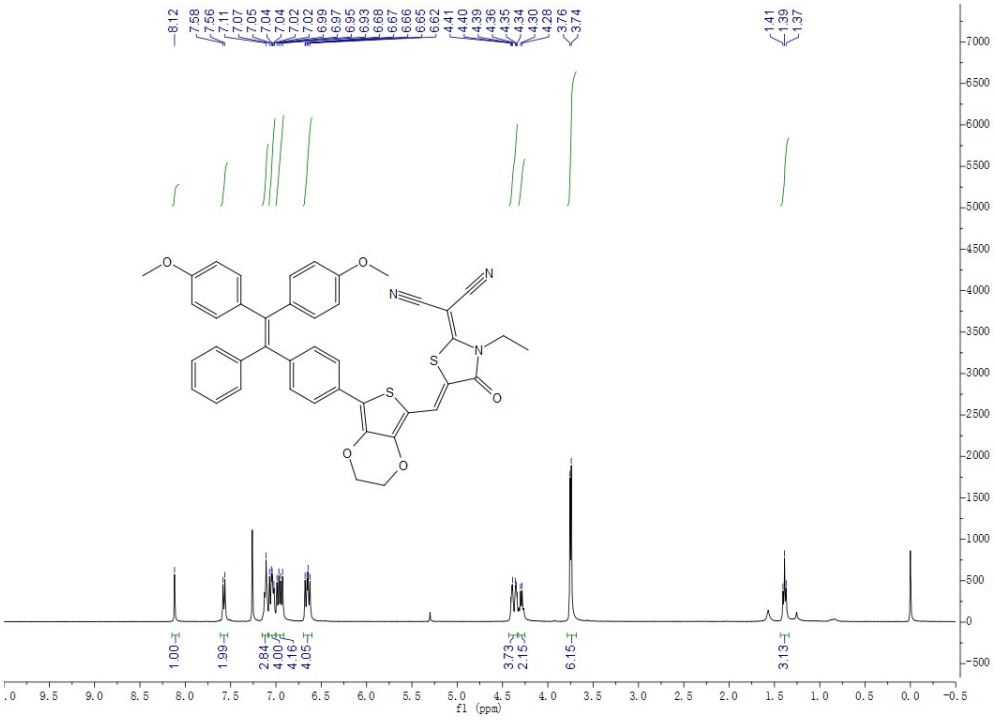

Figure S4. ^{1}H NMR spectrum of **TETCN**.

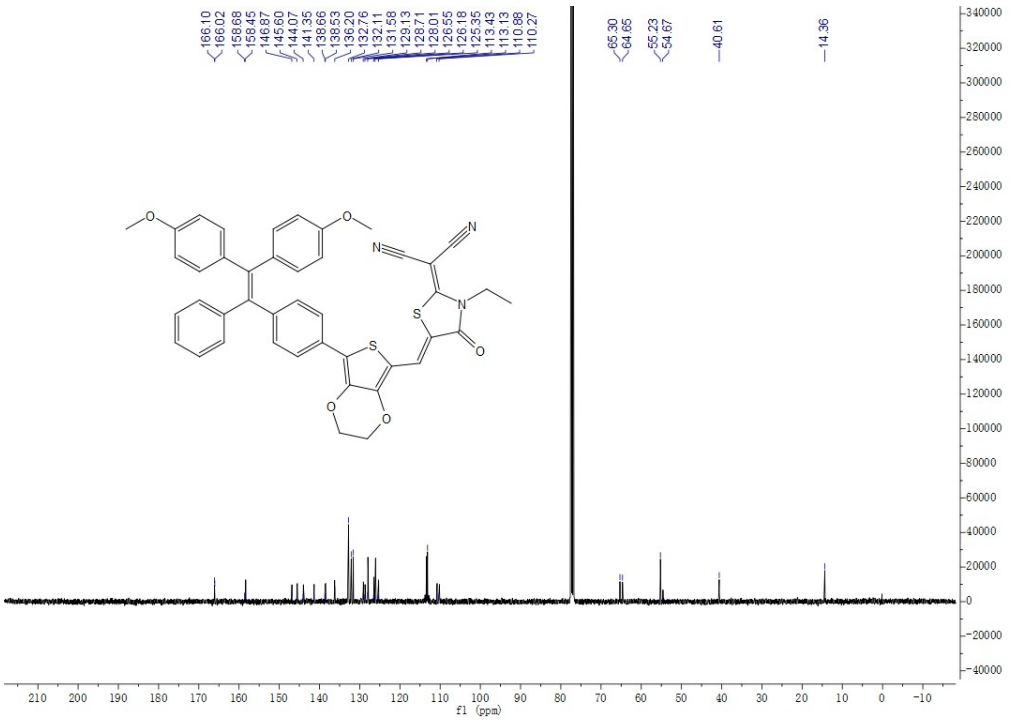

Figure S5. ^{13}C NMR spectrum of **TETCN**.

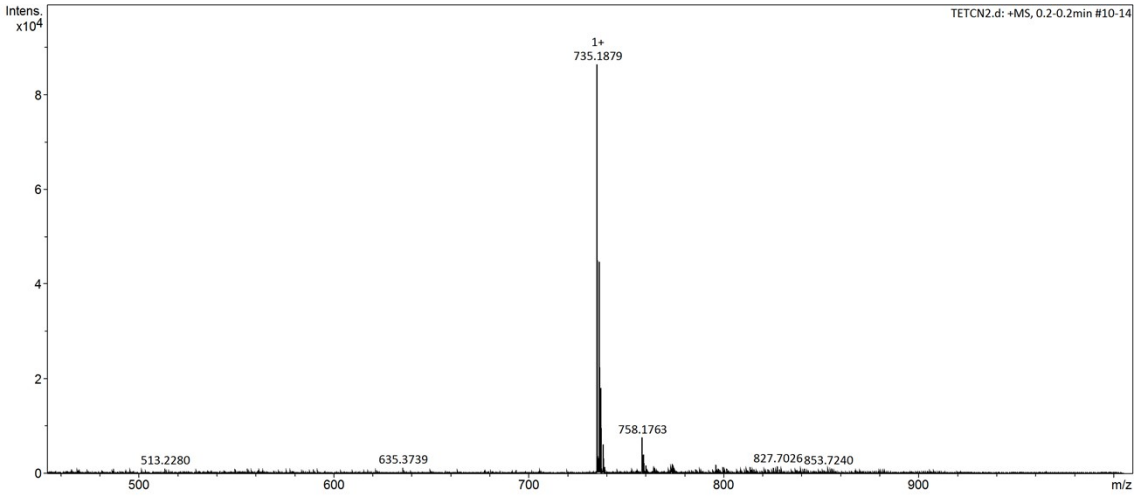

Figure S6. HR-MS spectrum of **TETCN**.

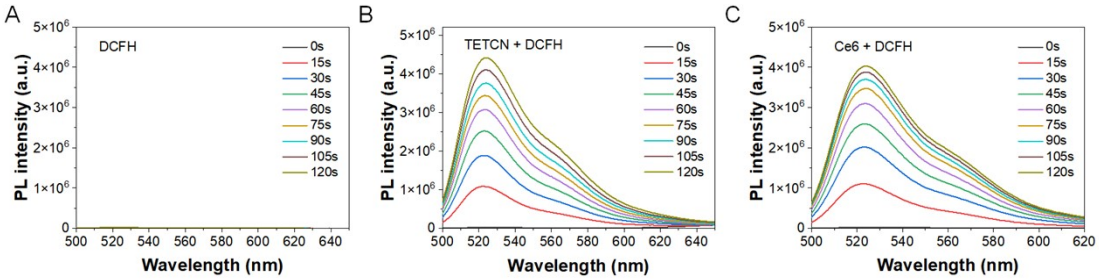

Figure S7. PL spectra of (A) DCFH (5 μM) alone or DCFH (5 μM) in the presence of (B) TETCN (10 μM) or (C) Ce6 (10 μM) in PBS under light irradiation (0.1 W cm^{-2}) for different times.

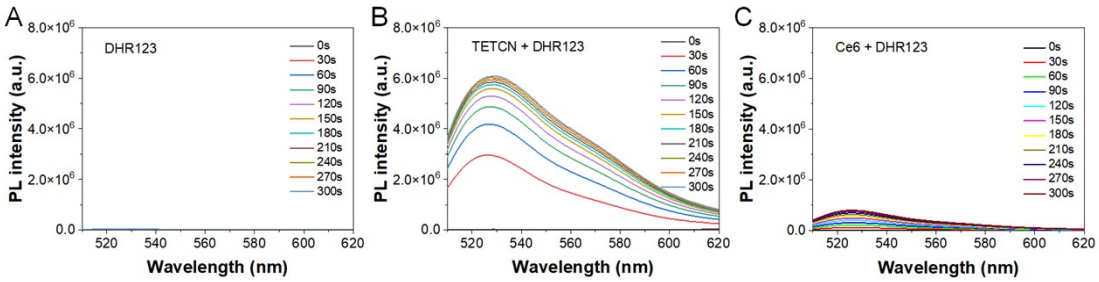

Figure S8. PL spectra of (A) DHR123 (5 μM) alone or DHR123 (5 μM) in the presence of (B) TETCN (10 μM) or (C) Ce6 (10 μM) in PBS under light irradiation (0.1 W cm^{-2}) for different times.

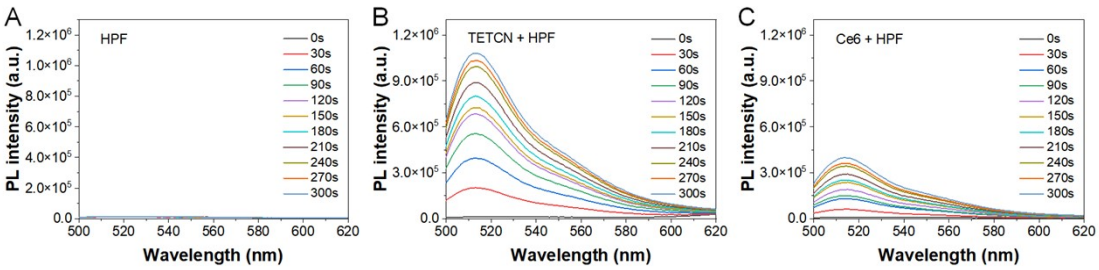

Figure S9. PL spectra of (A) HPF (5 μM) alone or HPF (5 μM) in the presence of (B) TETCN (10 μM) or (C) Ce6 (10 μM) in PBS under light irradiation (0.1 W cm^{-2}) for different times.

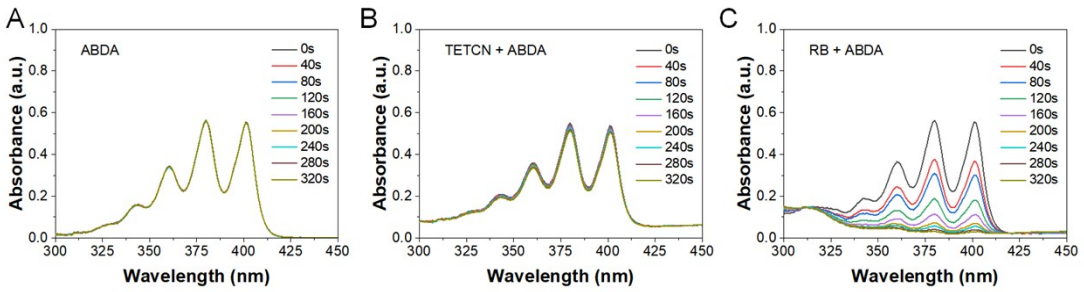

Figure S10. The absorbance of (A) ABDA (50 μM) alone or ABDA (50 μM) in the presence of (B) TETCN (10 μM) or (C) Ce6 (10 μM) in PBS under light irradiation (0.1 W cm^{-2}) for different times.

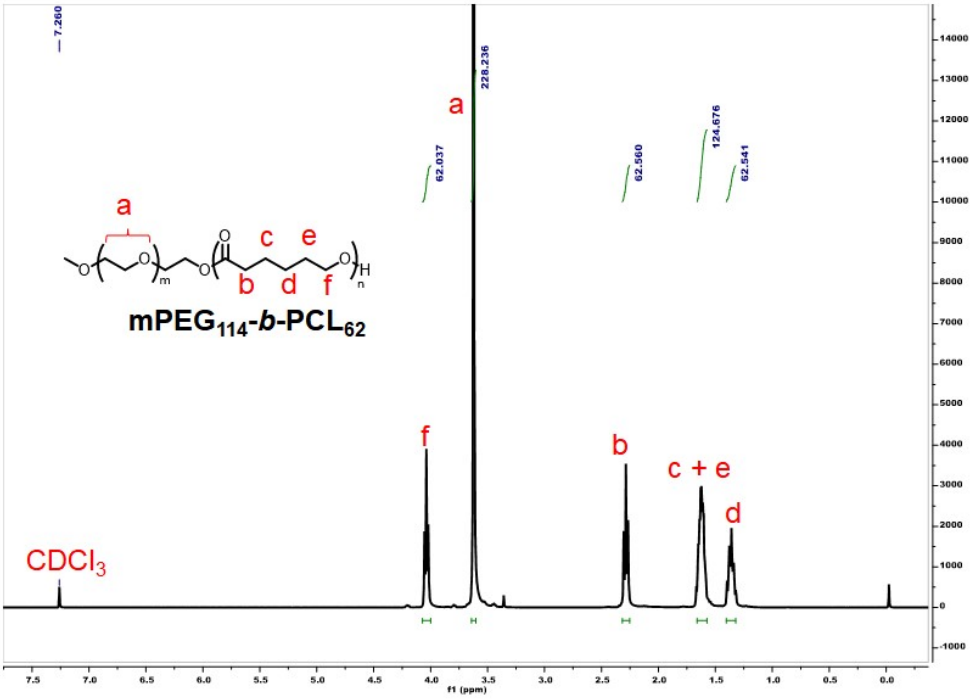

Figure S11. ^{1}H NMR spectrum of PCL-b-PEG.

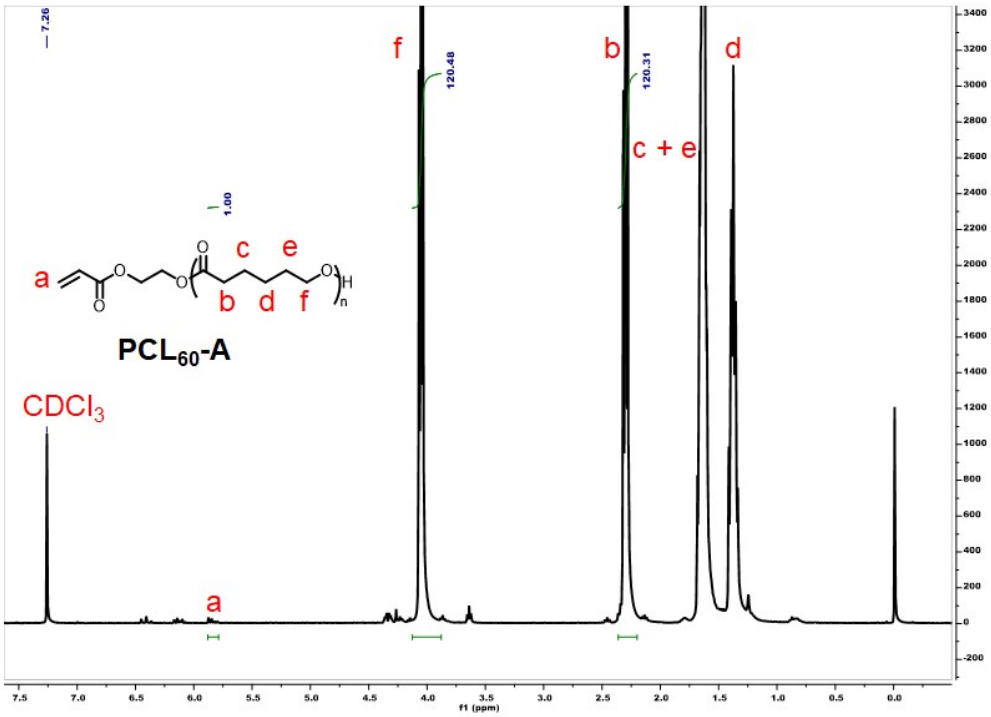

Figure S12. ^{1}H NMR spectrum of **PCL60-A**.

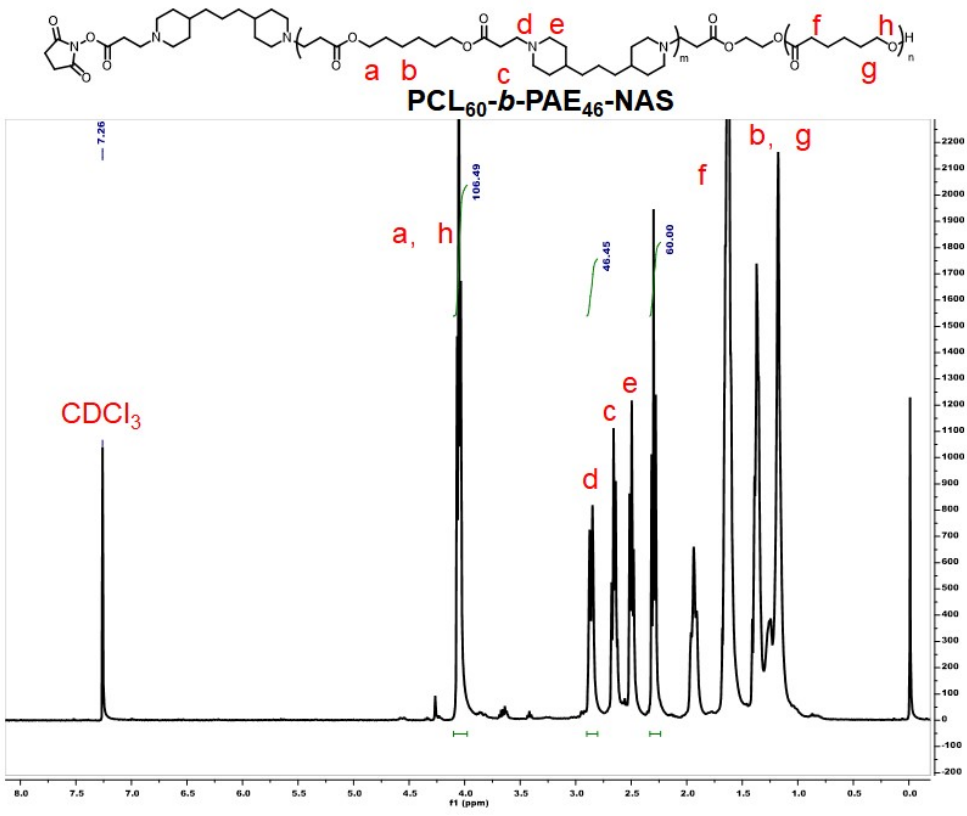

Figure S13. ^{1}H NMR spectrum of **PCL-b-PAE-NAS**.

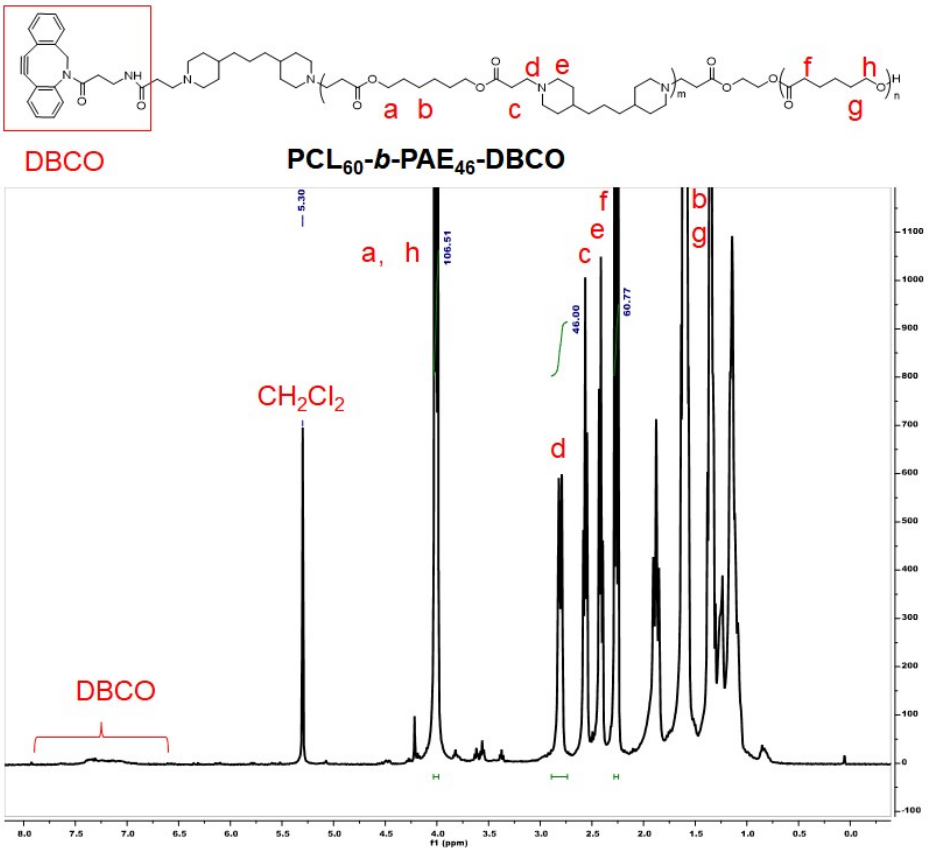

Figure S14. ^{1}H NMR spectrum of **PCL-b-PAE-DBCO**.

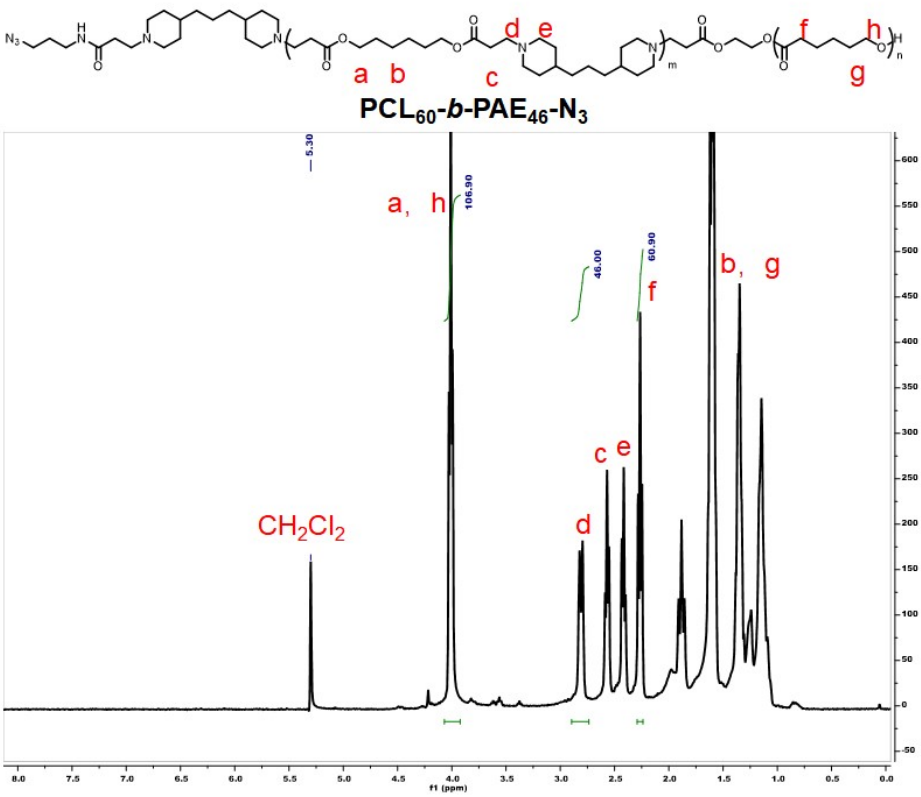

Figure S15.^{1}H NMR spectrum of **PCL-b-PAE-N_3**.

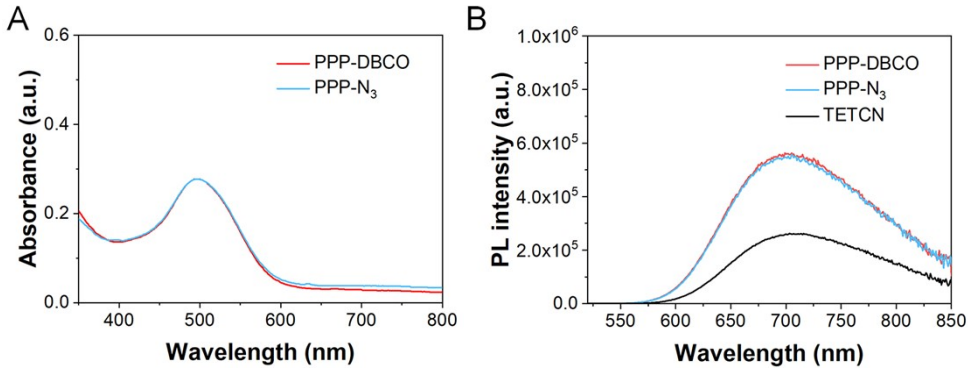

Figure S16. (A) The absorbance of PPP-DBCO and PPP-N_3 (containing 10 μM TETCN) in water. (B) The aggregation-induced emission (AIE) enhancement of TETCN before and after forming NPs (containing 10 μM TETCN) excited at 495 nm. For TETCN group, the solution was 95% water + 5% THF. For both NPs, the solution was pure water.

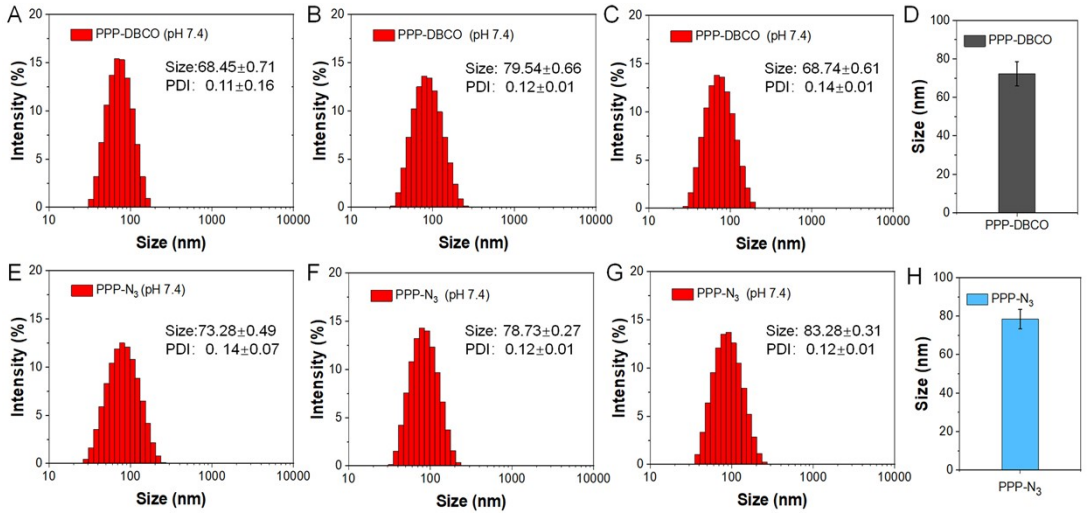

Figure S17. DLS size distributions of three batches of (A-C) PPP-DBCO and (E-G) PPP-N_3. (D) The particle size distribution statistics from A-C. (H) The particle size distribution statistics from E-G.

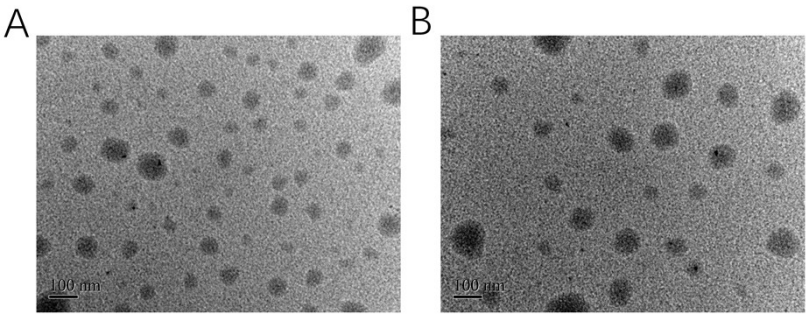

Figure S18. Representative TEM images of (A) PPP-DBCO and (B) PPP-N_3 at pH 7.4.

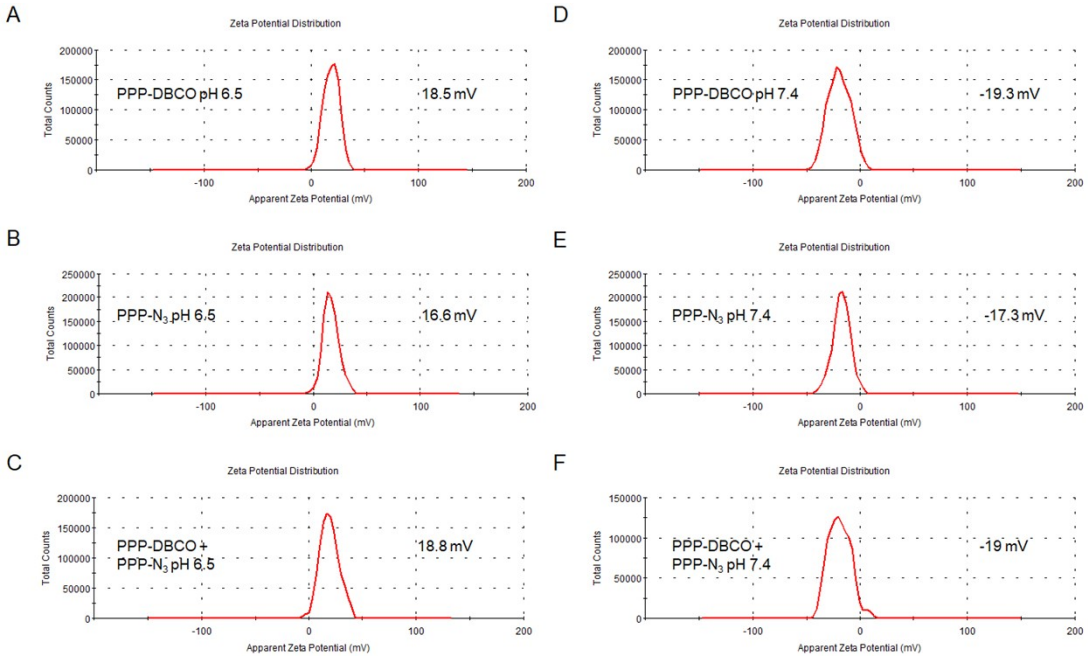

Figure S19. (A-F) Line graph of nanoparticles in aqueous solution (A) PPP-DBCO (pH 6.5), (B) PPP-N_3 (pH 6.5), (C) PPP-DBCO + PPP-N_3 (pH 6.5), (D) PPP-DBCO (pH 7.4), (E) PPP-N_3 (pH 7.4), (F) PPP-DBCO + PPP-N_3 (pH 7.4).

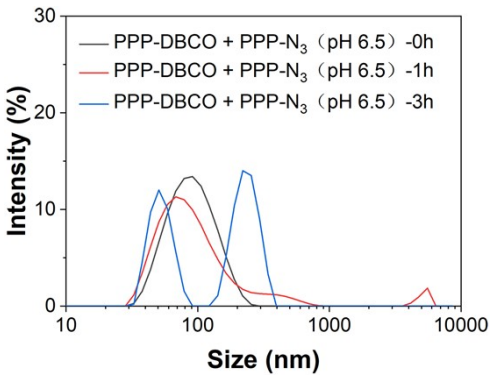

Figure S20. DLS results of the mixed NPs at pH 6.5 at different time.

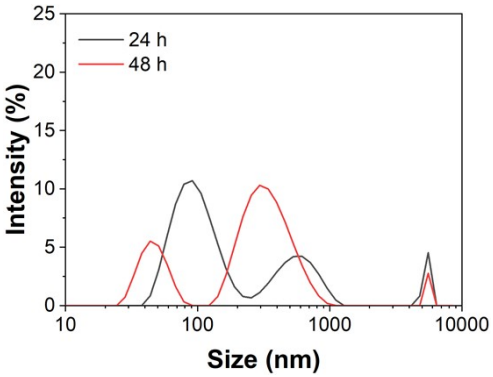

Figure S21. The stability of the cross-linked particles in PBS (pH 7.4) with 10% FBS

at 24 and 48 h. The cross-linked particles were prepared by mixing PPP-DBCO and PPP-N_3 in water at pH 6.5 for 5 h in advance.

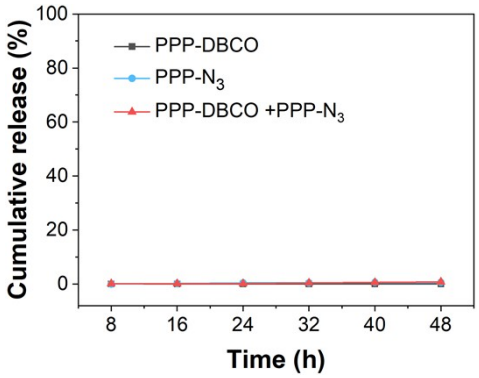

Figure S22. The cumulative release of TETCN of PPP-DBCO, PPP-N_3 and cross-linked PPP-DBCO + PPP-N_3 in water at pH 6.5.

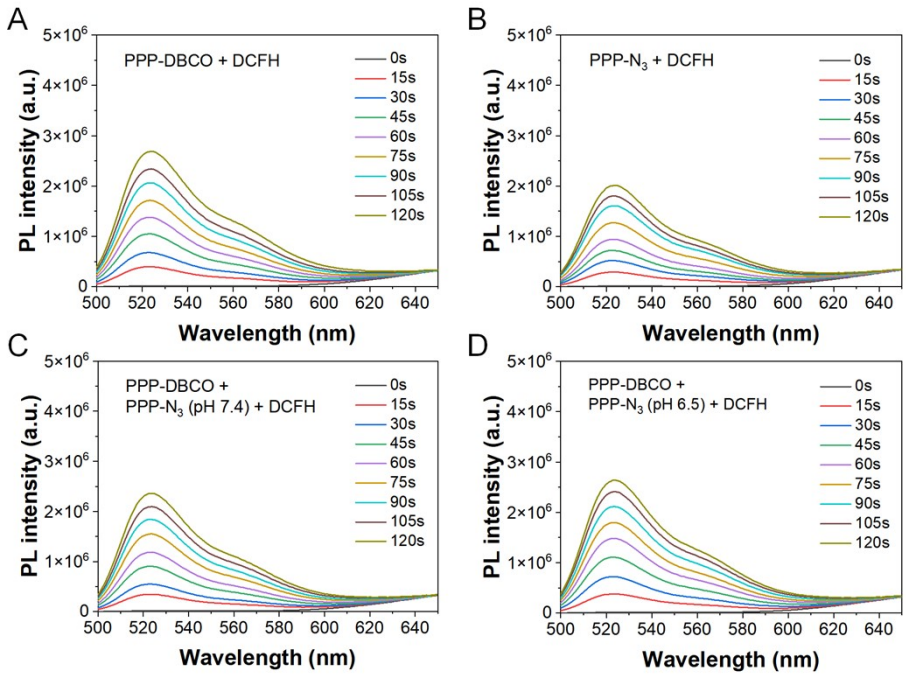

Figure S23. PL spectra of DCFH in the presence of (A) PPP-DBCO, (B) PPP-N_3, (C) PPP-DBCO + PPP-N_3 (pH 7.4), and (D) PPP-DBCO + PPP-N_3 (pH 6.5) in PBS under the irradiation (0.1 W cm^{-2}) with different irradiation times. [AIE NPs] =10 μM, [DCFH] = 5 μM.

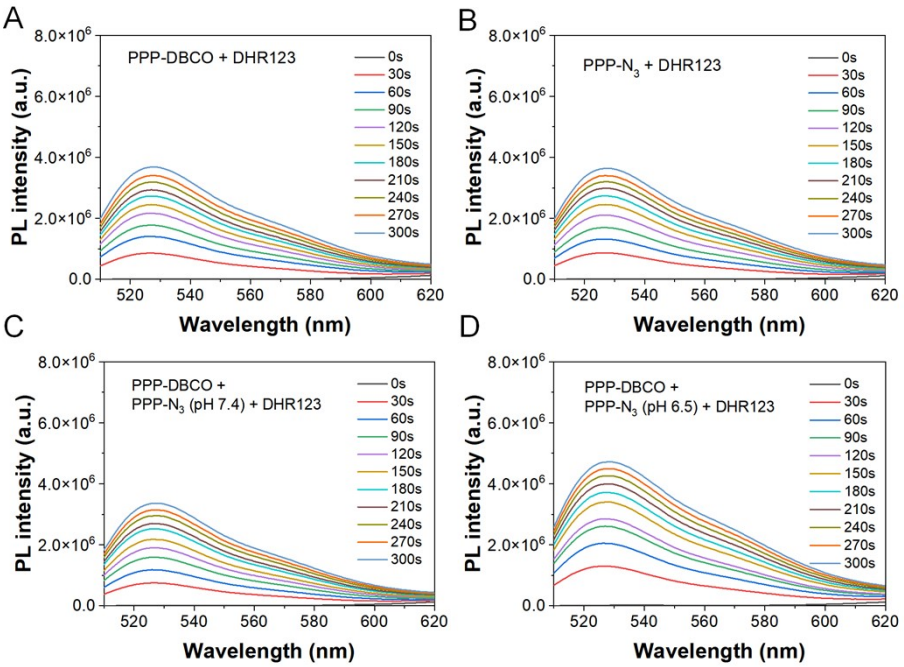

Figure S24. PL spectra of DHR123 in the presence of (A) PPP-DBCO, (B) PPP-N_3, (C) PPP-DBCO + PPP-N_3 (pH 7.4), and (D) PPP-DBCO + PPP-N_3 (pH 6.5) in PBS under the irradiation (0.1 W cm^{-2}) with different irradiation times. [AIE NPs] =10 μM, [DHR123] = 5 μM.

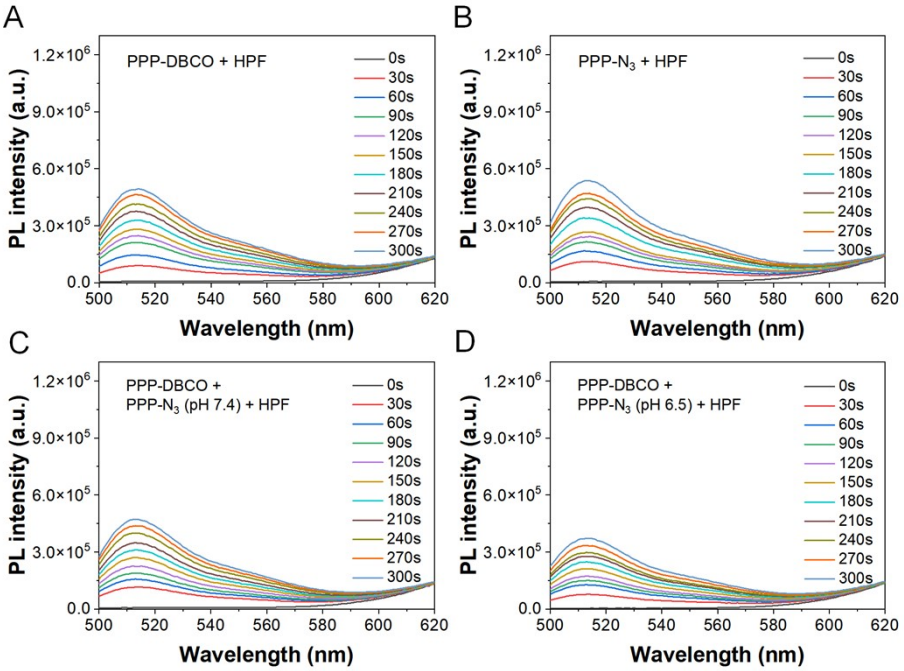

Figure S25. PL spectra of HPF in the presence of (A) PPP-DBCO, (B) PPP-N_3, (C) PPP-DBCO + PPP-N_3 (pH 7.4), and (D) PPP-DBCO + PPP-N_3 (pH 6.5) in PBS under the irradiation (0.1 W cm^{-2}) with different irradiation times. [AIE NPs] =10 μM, [HPF]

= 5 μM.

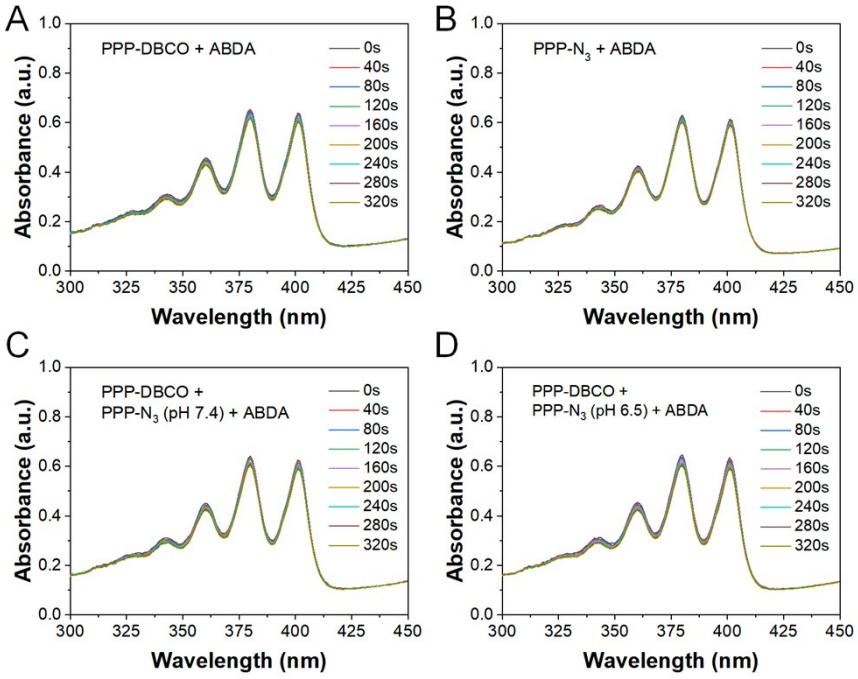

Figure S26. The absorbance of ABDA in the presence of (A) PPP-DBCO, (B) PPP-N_3, (C) RB, (D) PPP-DBCO + PPP-N_3 (pH 7.4), and (E) PPP-DBCO + PPP-N_3 (pH 6.5) under light irradiation (0.1 W cm^{-2}). [AIE NPs] =10 μM, [ABDA] = 50 μM.

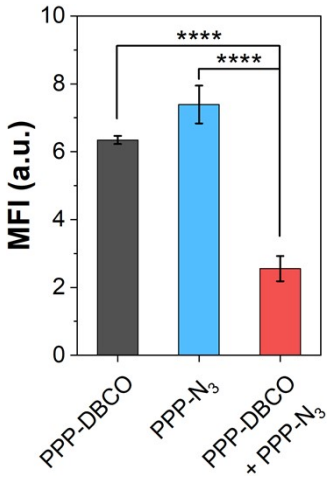

Figure S27. The mean fluorescence intensity (MFI) of 4T1 cells incubated with various NPs for 8 h. For PPP-DBCO + PPP-N_3 group, the NPs had been stirred in a pH 6.5 solution in advance to form large aggregates. Error bars: mean ± SD (n=3). The one-way ANOVA test was used for statistical analysis (****$p<0.0001$).

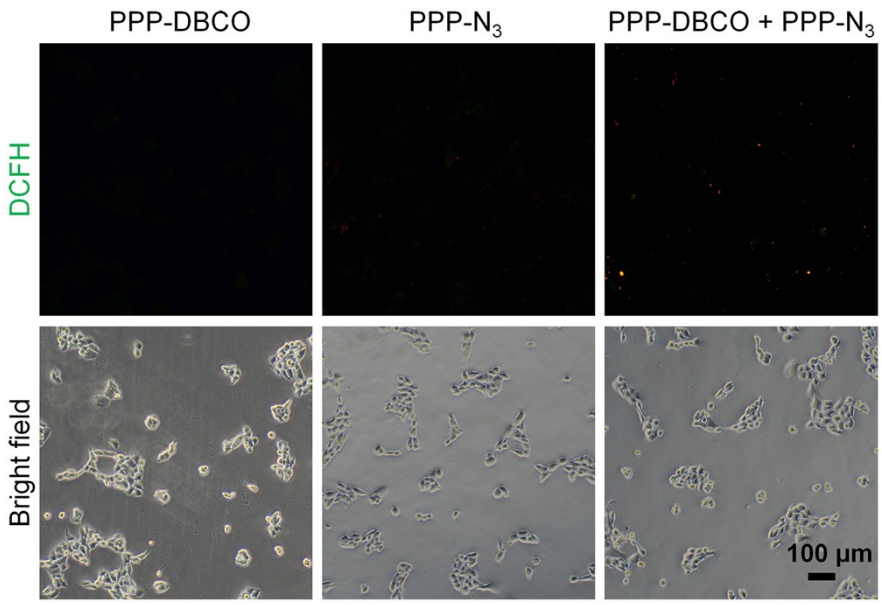

Figure S28. The intracellular ROS detection of 4T1 cells incubated with PPP-DBCO (20 μM), PPP-N_3 (20 μM) or PPP-DBCO + PPP-N_3 (20 μM) for 8 h under dark.

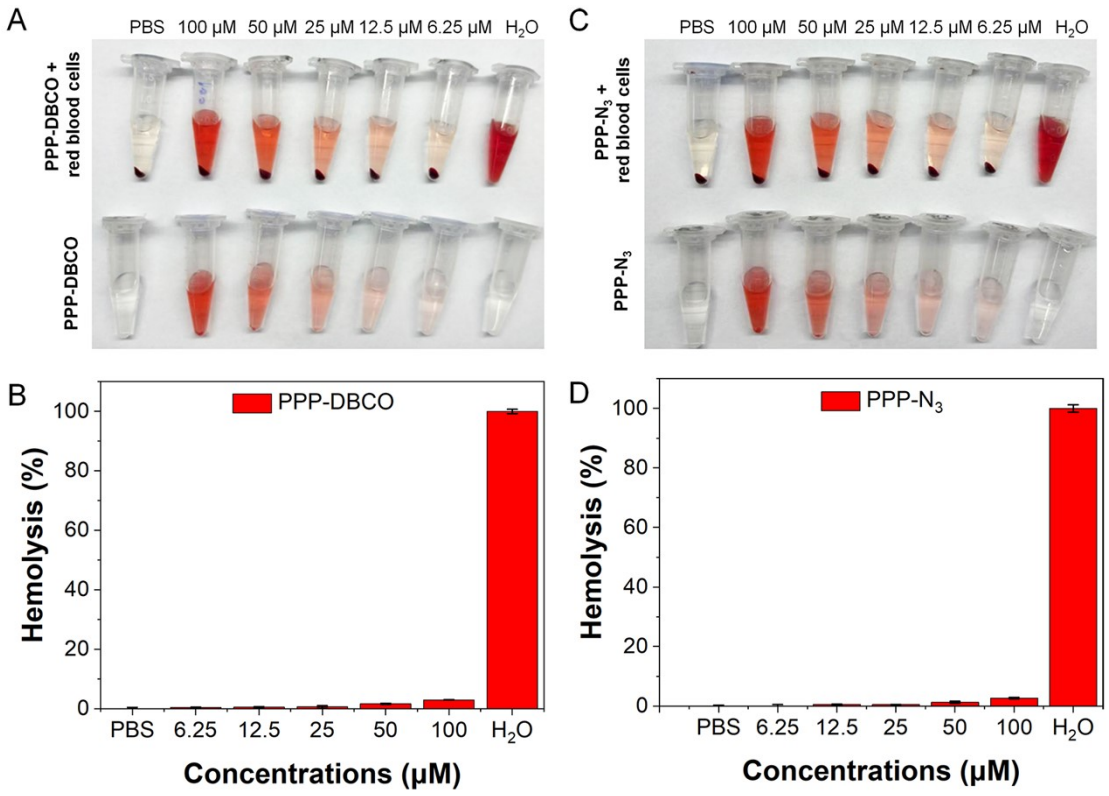

Figure S29. Hemolysis of (A-B) PPP-DBCO and (C-D) PPP-N_3 NPs after incubation with red blood cells with various concentrations, where PBS and H_2O were used as negative and positive controls, respectively.

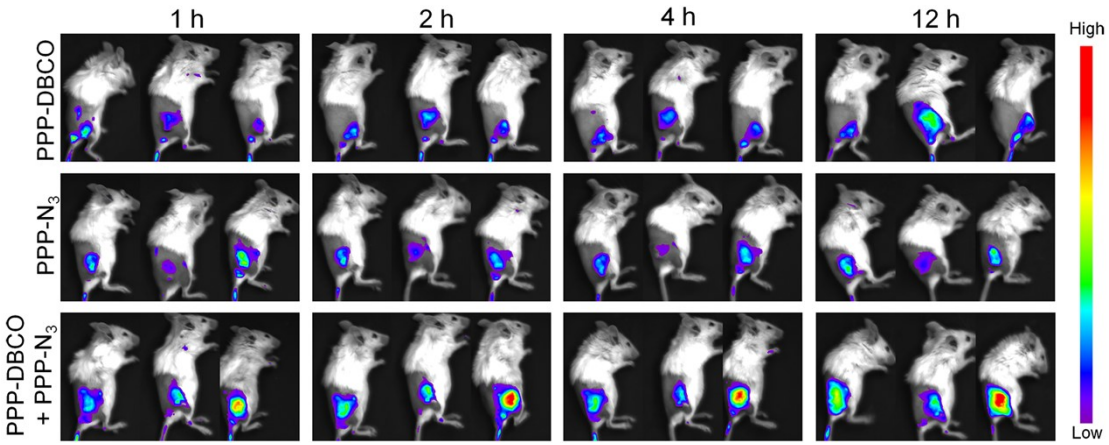

Figure S30. In vivo fluorescence images of 4T1 tumor-bearing mice intravenously injected with PPP-DBCO (1 mg/mL, 200 μL), PPP-N_3 (1 mg/mL, 200 μL) or PPP-DBCO (1 mg/mL, 100 μL) + PPP-N_3 (1 mg/mL, 100 μL) at different time points.

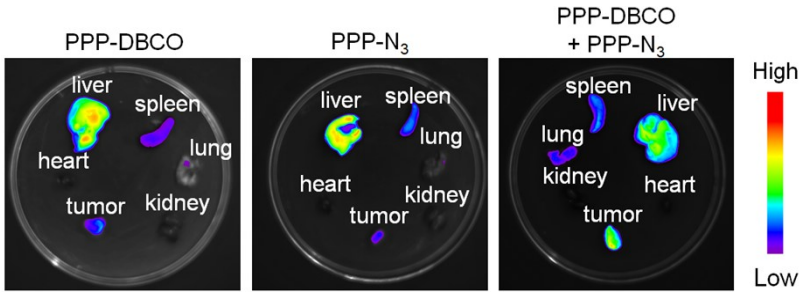

Figure S31. Ex vivo fluorescence images of main organs and tumors of 4T1 tumor-bearing mice intravenously injected PPP-DBCO (1 mg/mL, 200 μL), PPP-N_3 (1 mg/mL, 200 μL) or PPP-DBCO (1 mg/mL, 100 μL) + PPP-N_3 (1 mg/mL, 100 μL) for 24 h.

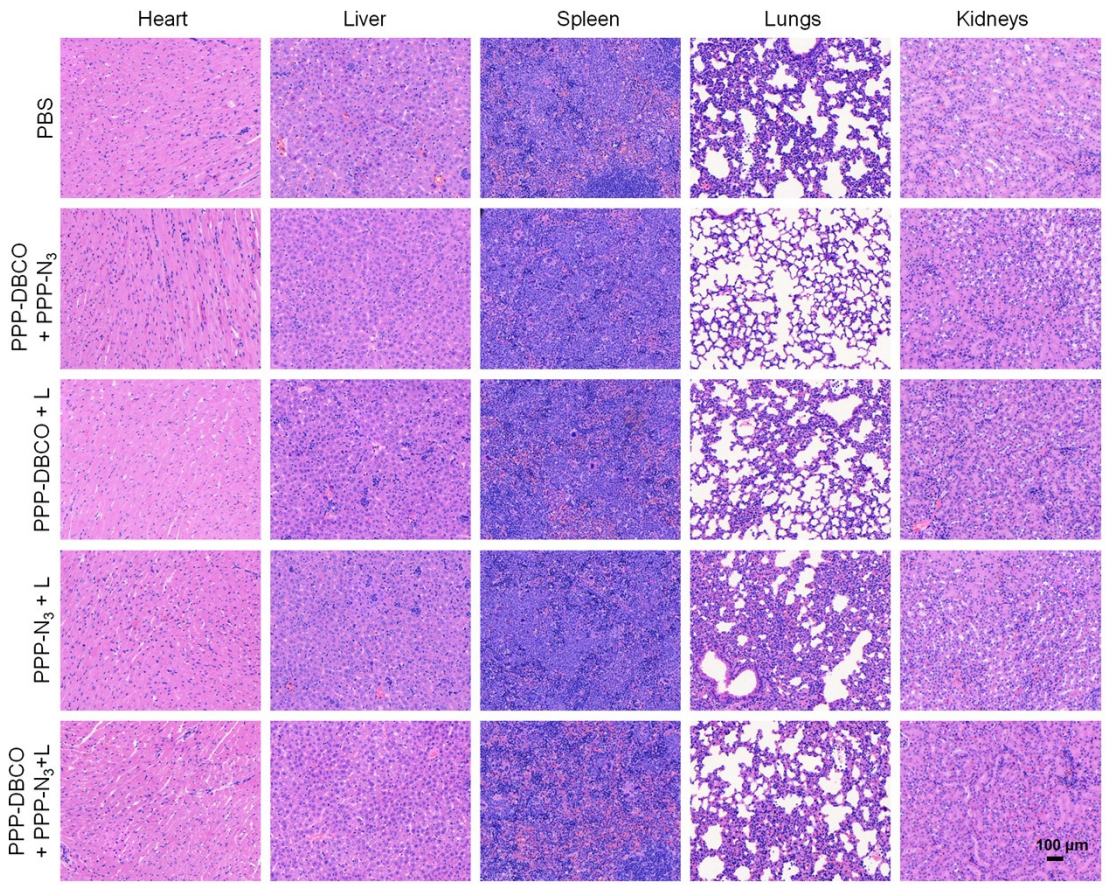

Figure S32. H&E staining images of 4T1 tumor tissues and major organ slices on day 14 post-treatment.

References:

1. H. Liu, W. Wang, Y. Zhou and Z. a. Li, *Journal of Materials Chemistry A*, 2021, **9**, 1080-1088.
2. L. Li, G. Yuan, Q. Qi, C. Lv, J. Liang, H. Li, L. Cao, X. Zhang, S. Wang, Y. Cheng and H. He, *Journal of Materials Chemistry B*, 2022, **10**, 3550-3559.
3. Y. Zhang, H. Fu, J. Chen, L. Xu, Y. An, R. Ma, C. Zhu, Y. Liu, F. Ma and L. Shi, *Small Methods*, 2023, **7**, 2201051.
4. N. Niu, Y. Yu, Z. Zhang, M. Kang, L. Wang, Z. Zhao, D. Wang and B. Z. Tang, *Chemical Science*, 2022, **13**, 5929-5937.